A computational study of oxide ion migration and water incorporation in the cuspidine system, $La_4(Ti_2O_8)O_2$

E. Kendrick*, M. Russ, and P.R. Slater

Chemistry, University of Surrey, Guildford, Surrey. GU2 7XH. UK

Correspondence to: Dr. E. Kendrick

Chemistry, University of Surrey, Guildford, Surrey. GU2 7XH. UK

Tel. +44 1483 689591 Fax +44 1483 686851

e-mail: e.kendrick@surrey.ac.uk

Abstract

The cuspidine system, $La_4(Ti_{2-x}Ga_xO_{8-x/2})O_2$ has recently been shown to display significant oxide ion conductivity at elevated temperatures, with evidence for proton conduction at low temperatures in wet atmospheres. In this paper we present a computer modelling study of the $La_4(Ti_2O_8)O_2$ (x=0) end-member. In agreement with experimental studies, the most favourable oxide ion vacancy defect is found at the bridging oxygen position (O3). Oxide ion migration is shown to proceed via a cooperative vacancy migration process with a calculated activation energy of 1.51 eV, in very good agreement with experiment. The computational results for water incorporation suggest that oxygen vacancies are required for water incorporation to occur, which also agrees with experiment, and the most favourable position for the proton is the bridging oxygen (O3).

Keywords: Oxide ion conduction, proton conduction, cuspidine.

PACS: 66.30.Dn

1. Introduction

Materials displaying high oxide-ion and proton conductivity have attracted considerable interest due to technological applications in solid oxide fuel cells (SOFCs), sensors and separation membranes. Traditionally fluorite and perovskite-related materials have been targeted, although more recently there has been growing interest in alternative structure types, such as $La_2Mo_2O_9$, apatites, and cuspidines [1-5]. The complex structures of these new materials raises the key question of how oxide ion/proton migration proceeds. In this respect, computer modelling studies can provide important information, as shown for the apatite-type lanthanum silicates, where a complex interstitial migration mechanism was identified [6]. In this paper we perform similar atomistic simulation studies for the cuspidine systems. Research in this area has grown following the initial report of oxide ion conduction in $Nd_4(Ga_{2-x}M_xO_{7+x/2})O_2$ (M=Ti, Ge) by Joubert *et al.* [7,8] Subsequently Martin-Sedeno *et al.* confirmed these results, and showed that in the system, $La_4(Ga_{2-x}Ti_xO_{7+x/2})O_2$ proton conduction was also observed at low temperatures (below ≈950K) in wet atmospheres [9, 10].

Cuspidine-type oxides have the ideal general formula $A_4(M_2O_7)O_2$ (A= rare earth, M= Al, Ga) and can be described as consisting of chains of edge-sharing AO_7/AO_8 polyhedra interconnected through the M_2O_7 units. As shown by the earlier work in this area, the formula is better written as $A_4(M_2O_7\square_1)O_2$ (□= oxygen vacancy) to show that there is a vacant oxygen position between the M_2O_7 groups [9]. By suitable doping with a higher valent cation, e.g. $La_4(Ga_{2-x}Ti_xO_{7+x/2}\square_{1-x/2})O_2$, the introduction of extra oxygen is possible, leading to the conversion of the isolated M_2O_7 groups into infinite chains of distorted trigonal bipyramids, as observed for $La_4(Ti_2O_8)O_2$ (figure 1) [10].

In order to investigate the defect characteristics and ion migration mechanisms in these cuspidine systems in more detail, we report an atomistic simulation study of $La_4(Ti_2O_8)O_2$.

2. Methods

The structure and defects in the cuspidine type $La_4(Ti_2O_8)O_2$ were investigated with atomistic potential energy minimisation computer simulations [11]. This atomistic potential method utilises energy minimisation techniques to determine the lowest energy configuration of the crystal system with respect to the atomic positions. The potential energy of the crystal lattice is obtained by summing the long range Coloumbic terms and the short range repulsion and dispersion forces or pair potentials, in this case the atomistic pair potentials are in the form of the Buckingham Potential (Eq 1).

$$V_{ij} = A_j \exp\left(\frac{-r}{\rho_{ij}}\right) - \frac{C_{ij}}{r^6} \qquad (1)$$

An important feature of the model is the ability to describe the polarisation of the atoms and in this system both the lanthanum and oxygen atoms are described in terms of the shell model: an atomic shell of charge Y, which represents the valence electrons, is connected to the atomic core or core electrons by a harmonic spring constant k. The polarisability on the free ion can therefore be described as:

$$\alpha = Y^2/k \qquad (2)$$

For the water incorporation studies, the O-H interaction is modelled using the Morse potential:

$$V(r) = D\{1 - \exp[-\beta(r - r_0)]\}^2 \qquad (3)$$

The potentials were fitted to experimental data [10], and good agreement to the structure was obtained. The Buckingham potentials and shell charges used in the model for $La_4(Ti_2O_8)O_2$ and the comparison to the experimental structure are given in table 1. The defects are modelled with the Mott-Littleton approach [12] where the region around the defect is split into two regions. The inner region is a specified radius, in this case 12Å, and the outer region stretches to infinity. The relaxation of the inner region is calculated explicitly, while the atoms

in the outer regions are relaxed by quasi-continuum methods. A more detailed description of this technique has been given elsewhere [13].

3. Results and Discussion

Structure and Defects

The structure of $La_4(Ti_2O_8)O_2$ is composed of chains of TiO_5 groups, which are bridged by oxygens (O3), with channels of lanthanum and oxygen sandwiched between the chains (figure 1). Initially, the Frenkel and Schottky defect energies were calculated (Table 2), with the most favourable intrinsic defect energy being the oxygen Frenkel defect (1.41 eV/defect). This is relatively low compared to the Lanthanum and Titanium Frenkel defect energies, and suggests that low levels of interstitia1 oxygen ions may occur in these materials at higher temperatures. This phenomenon may account for the presence of high temperature oxide ion conduction in stoichiometric $La_4(Ti_2O_8)O_2$ and an interstitial oxide ion conduction migration mechanism is discussed below. The most favourable interstitial position was found to be located directly below the titanium in the trigonal pyramid TiO_5, forming an octahedral unit (Figure 2a). The lowest energy for an oxygen vacancy occurs at the O3 bridging site (Figure 2b). This defect creates a break in the TiO_5 chains forming two terminal TiO_4 groups, similar to the structure observed for $La_4(Ga_2O_7)O_2$. [9]

Oxide ion migration mechanisms

In order to elucidate the oxide ion diffusion mechanisms in this material, initial oxide ion vacancy diffusion pathways between adjacent O3 sites were attempted. This proved to be a non trivial task, with several vacancy migration pathway calculations between adjacent sites proving unsuccessful. A different ‘co-operative’ oxide ion movement, rather than the common vacancy ‘hopping’ mechanism, which is observed for perovskites and fluorites was therefore considered. Nudged elastic band calculations (NEB) were used to calculate

rotational trajectories of the oxygens around the titanate units. These calculations were performed by creating an oxygen vacancy point defect at an O3 position, and then using the nudged elastic band technique to rotate two oxygens, one into the vacancy position and one into the position just vacated, creating an O3 vacancy at the adjacent O3 position. The most favourable rotation occurs via such a co-operative vacancy hopping mechanism (Figure 3a), where a bridging oxygen (O3) rotates towards an O2 position, as the O2 oxygen moves in a co-operative motion towards the vacant oxygen site. An energy barrier of 1.51eV was calculated for this mechanism, which is in excellent agreement with the experimentally observed values for oxygen deficient $La_4(Ti_{2-x}Ga_xO_{8-x/2})O_2$ systems ($E_a \approx 1.6$ eV) [10]. The lower valence of Ga compared to Ti could in principle result in some Ga-oxygen vacancy defect association. However, the fact that there is only a small difference between the experimental activation energy (1.6 eV) and that calculated from the modelling (1.51 eV) would suggest that any defect association is small.

The energy barrier for interstitial oxide ion migration was then investigated, using the same structure as for the vacancy migration, and was found to be low (0.49eV) compared to the vacancy migration. However, in order for an interstitial migration mechanism to occur in $La_4(Ti_2O_8)O_2$, a Frenkel defect must first be created, which requires additional energy. This would explain the lower conductivities in undoped $La_4(Ti_2O_8)O_2$, but also poses the question whether oxygen excess systems can be prepared by suitable doping, as an alternative means of enhancing the conductivity. Further experimental strudies are required to investigate this possibility. Figure 3b shows the interstitial migration mechanism, which propagates via the movement of the interstitial oxide ion along the TiO_5 chain.

Proton Incorporation

As shown by Martin-Sedeno *et al.*, water incorporation and proton conduction can occur in these cuspidine systems at low temperatures [10]. The defect energy for an OH defect has

therefore been calculated for a proton attached to different oxygen atoms within the structure and at the most favourable oxygen interstitial position. The calculations indicate that the most favourable site for proton incorporation is at the O3 bridging oxygen. The equations and energies for the water incorporation at a vacant O3 site and the interstitial positions are given in table 3. The higher water incorporation energies at interstitial and mixed interstitial and vacant sites suggest that oxygen vacancies are required for water incorporation to occur. This result agrees with experimental data where proton conduction has been only observed in the materials which possess oxide ion vacancies [10]. Further studies are required to elucidate the proton conduction mechanism.

4. Conclusions

$La_4(Ti_2O_8)O_2$ possesses a complex cuspidine-type structure, and as a result a more in depth NEB method of investigation was necessary to elucidate oxide ion conduction mechanisms and processes. This NEB method highlights the importance of co-operative oxygen movement in this material, with the most favourable oxide ion vacancy mechanism being for a co-operative rotational process, which propagates the vacancy from one O3 bridging position to the next. The calculated activation energy of 1.51 eV corresponds well to experimental data. The most favourable position for water incorporation was shown to be at the oxygen vacancy sites, rather than at an interstitial position, indicating that vacancies are required for water incorporation in agreement with experiment. Overall, this work illustrates the power of atomistic potential modelling in aiding our understanding of defects and defect processes at the atomic level in complex systems such as this.

References

1. J.B. Goodenough, *Annu. Rev. Mater. Res*. 33 (2003) 9.

2. K.D. Kreuer, *Ann. Rev. Mater. Res*. **33** (2003) 333.

3. P. Lacorre, F. Goutenoire, O. Bohnke, R. Retoux, Y. Laligant; *Nature* 404 (2000) 856.

4. S. Nakayama, H. Aono, Y. Sadaoka, *Chem. Lett*. (1995) 431.

5. J.E.H. Sansom, D. Richings, P.R. Slater, *Solid State Ionics* 139 (2001) 205.

6. E. Kendrick, M.S. Islam, P.R. Slater; *J. Mater. Chem*. 17 (2007) 3104.

7. O. Joubert, A. Magrez, A. Chesnaud, M.T. Caldes, V. Jayaraman, Y. Piffard, L. Brohan; *Solid State Sci* 4 (2002) 1413.

8. A. Chesnaud, O. Joubert, M. Caldes, S. Gosh, Y. Piffard, L. Brohan; *Chem. Mater.* 16 (2004) 5372.

9. M.C. Martin-Sedeno, E.R. Losilla, L. Leon-Reina, S. Bruque, D. Marrero-Lopez, M.A.G. Aranda; *Chem. Mater*. 16 (2004) 4960.

10. M.C. Martin-Sedeno, D. Marrero-Lopez, E.R. Losilla, L. Leon-Reina, S. Bruque, P. Nunez, M.A.G. Aranda; *Chem. Mater*. 17 (2005) 5989.

11. J.D. Gale and A.L. Rohl, *Mol. Simul.* 29 (2003) 291

12. A. B. Lidiard, *Chem. Soc., Faraday Trans. 2,* 85 (1989) 341

13. *Computer Modelling in Inorganic Crystallography*. Ed. C. R. A. Catlow, Academic press, San Diego, CA, 1997.

Figure Captions

Figure 1. Structure of $La_4(Ti_2O_8)O_2$, white spheres = La, black spheres = Ti, and grey spheres = O.

Figure 2(a). Most favourable oxygen vacancy position in $La_4(Ti_2O_8)O_2$

(b) Most favourable oxygen interstitial position in $La_4(Ti_2O_8)O_2$

Figure 3(a). Vacancy hopping migration via rotation of the O2, and O3 oxygens, calculated by the nudged elastic band method.

(b) Proposed interstitial oxygen migration mechanism.

Table 1a) Potential parameters for atomistic simulations of $La_4(Ti_2O_8)O_2$

Buckingham	A (eV)	ρ (eV)	C (eV Å^{-6})	Y (e)	k (eV Å^{-2})
La-O	1545.21	0.3589	0	-0.25	145
Ti-O	754.2	0.389	0		
O-O	22764.0	0.149	17.879	-2.869	74.92
H-O	311.97	0.25	0		
Morse	D (eV)	β (Å^{-1})	r (Å^{-1})		
H-O	7.0525	2.1986	0.6485		

Table 1b Comparison of calculated and experimental structures

	Experimental	Calculated	Difference
a (Å)	11.00922	10.9699	-0.36%
b (Å)	11.4631	11.54245	0.69%
c (Å)	3.94327	3.890881	-1.33%
Vol (Å^3)	497.64	492.67	-1.00%

Table 2(a). Schottky and Frenkel Defect energies for $La_4(Ti_2O_8)O_2$

Frenkel

	Defect Energy (eV)	Per defect (eV)
O	2.84	1.42
La	11.22	5.61
Ti	14.63	7.31

Schottky-type

TiO_2	9.83	3.28
La_2O_3	8.10	1.62
$La_4(Ti_2O_8)O_2$	28.47	1.78

Table 3: Water incorporation energies

Water incorporation equation	eV
$H_2O + V_o^{\bullet\bullet} + O_o \leftrightarrow 2OH_o^{\bullet}$	-0.12
$H_2O + V_i^{x} + O_o \leftrightarrow OH_o^{\bullet} + OH_o'$	1.84
$H_2O + V_i^{x} + O_i'' \leftrightarrow 2OH_i^{'}$	0.95

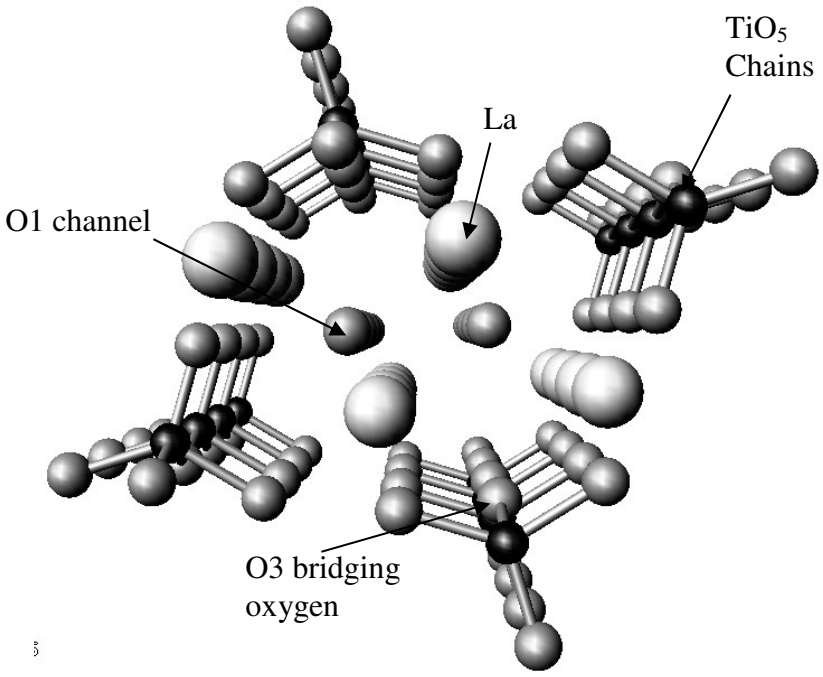

Fig 1.

Fig 2 a

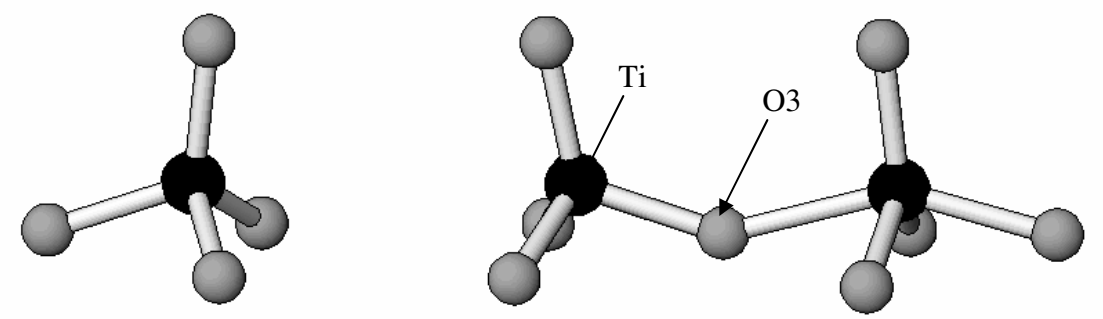

Fig. 2b

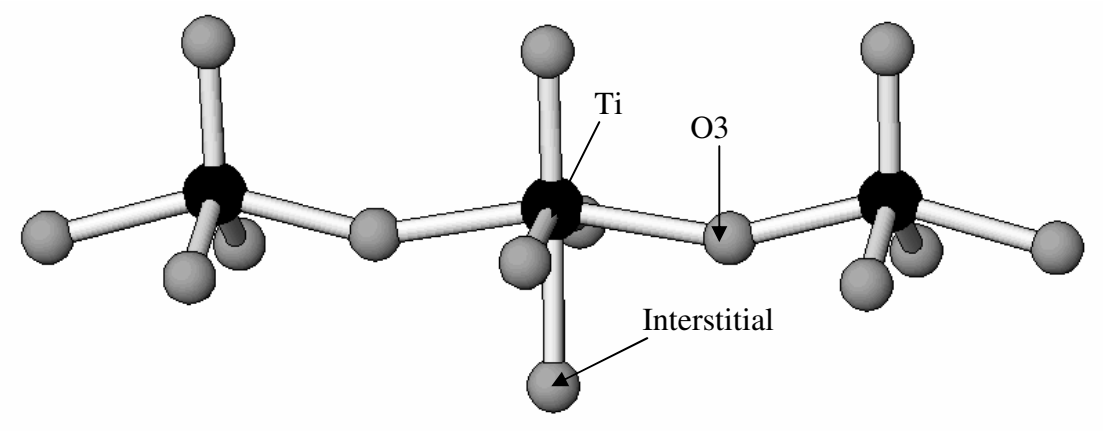

Fig 3a

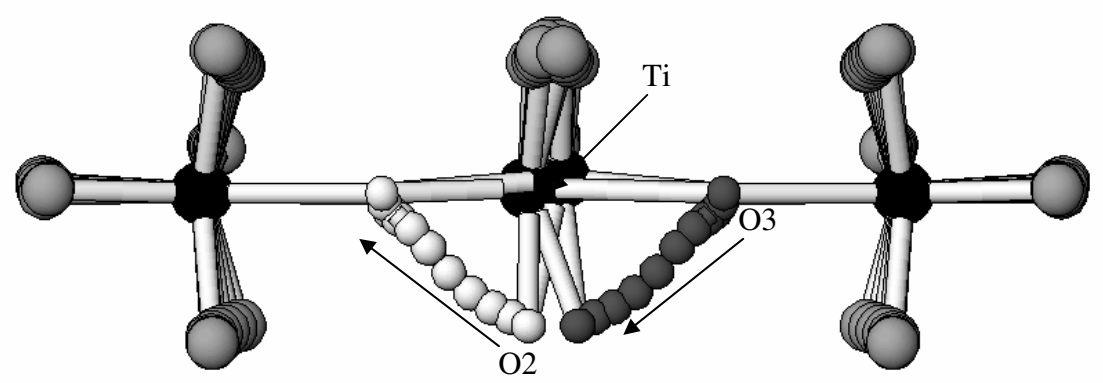

Fig. 3b